45th Aerospace Sciences Meeting & Exhibit
January 8-11, 2007 Reno, NV
AIAA-2007-0086

Aircraft Performance Sensitivity to Icing Cloud Conditions

Scot E. Campbell[1], Andy P. Broeren[2], and Michael B. Bragg[3]
University of Illinois at Urbana-Champaign, Urbana, IL 61801

and

Dean R. Miller[3]
NASA Glenn Research Center, Cleveland, OH 44135

The question of "How good is good enough?" has yet to be fully answered in regard to the accuracy of simulated icing conditions. This paper addresses this question in the form of an aerodynamic performance sensitivity to icing cloud parameter variations. Ice tracings were taken from an existing NASA study that examined the effects of icing parameter variations on ice accretion geometry. These ice accretions were simulated using SLA, and then aerodynamic testing was conducted at the University of Illinois subsonic wind tunnel. A sensitivity of aerodynamic performance to icing parameter variations was formed by relating the aerodynamic results of this test to the corresponding icing cloud parameter variations of the NASA study. To judge the real-world effect of icing cloud parameter variations, this sensitivity was extended from airfoil performance to aircraft performance. For the conditions of this study, it was found that if V_{stall} was required to be known within ±0.5 knots, the required accuracy in LWC was ±0.025 g/m^3, and in MVD was ±1.1 µm. For ΔV_{stall} = ±3 knots, the required accuracy in LWC was ±0.12 g/m^3, and in MVD was ±5.5 µm.

Nomenclature

α	angle of attack
C_d	airfoil drag coefficient
C_{dmin}	airfoil minimum drag coefficient
C_l	airfoil lift coefficient
C_{Lmax}	clean aircraft maximum lift coefficient
$C_{Lmax,ice}$	iced aircraft maximum lift coefficient
C_{lmax}	airfoil maximum lift coefficient
C_m	airfoil quarter-chord pitching moment coefficient
k/c	height of ice horn normalized by chord length
L/D	lift to drag ratio
$(L/D)_{max}$	maximum lift to drag ratio
LWC	liquid water content
S	wing planform area
S_{iced}	wing planform area containing a leading-edge ice accretion
s/c	location of ice horn along airfoil surface normalized by chord length
MVD	median volume diameter
V_{stall}	1g stall speed

I. Introduction

Aircraft icing is widely recognized as a significant hazard to aircraft operations. During the years 1990 to 2005, there were 33,513 aircraft accidents and incidents in the United States (US) that were reported in the National

[1] Graduate Research Assistant, Department of Aerospace Engineering.
[2] Research Scientist, Department of Aerospace Engineering, Senior Member AIAA.
[3] Professor, Department of Aerospace Engineering, Associate Dean for Research and Administrative Affairs, Fellow AIAA.
[4] Aerospace Engineer, Icing Branch, Member AIAA.

Transportation Safety Board (NTSB) accident database.[1] Out of these 33,513 accidents and incidents, 588 were related to flight into icing conditions. Of the accidents involving structural icing, 14 occurred during Part 121 (scheduled) operations, and 74 occurred during Part 135 (on-demand) operations. According to the database, the effects of icing are not limited to smaller aircraft. Transport category aircraft including mid-size jet aircraft, regional jets, and turboprops have all experienced problems with icing. The most recent incident involving a transport category aircraft occurred in a Saab 340B on January 2, 2006.[1] This aircraft encountered icing conditions, departed controlled flight at 11,500 MSL, and recovered at 6,500 MSL. The probable cause of this incident is still under investigation. The most recent fatal accident involving a transport category aircraft occurred on January 9, 1997.[1] In this accident an EMB-120 turboprop aircraft entered icing conditions and departed controlled flight on approach to Detroit Metropolitan Wayne County Airport. According to the NTSB, the accident was caused by an icing encounter in which the pilots experienced a "loss of control when the airplane accumulated a thin, rough, accretion of ice on its lifting surfaces." It is therefore critical to ensure that aircraft certification for flight into icing conditions is determined through the most accurate methods possible.

One method is to use an artificially generated ice accretion as a direct model for a simulated ice accretion. To simulate a natural ice accretion, an icing wind tunnel is used to accrete ice on a surface and then the ice accretion is either traced or molded to create a permanent representation. The ice tracing or mold is then used to manufacture the simulated ice accretion so that it can be used in dry-air testing. Icing wind tunnels simulate flight through icing conditions by using a water spray system to inject water into the cold air moving through the tunnel. The value of icing wind tunnels is their capability to control specific icing parameters such as liquid water content (LWC), median volume diameter (MVD), and temperature, which have a significant effect on ice accretion geometry. However, an unanswered question regarding simulation capabilities in icing wind tunnels is "how accurately do the icing parameters need to be controlled?" In other words, it is unknown to what accuracy icing parameters such as LWC and MVD need to be controlled so that the resulting simulated ice accretion is acceptable in terms of aerodynamically significant differences.

In 2005, Miller et al.[2] investigated the effect of icing parameter variations on ice accretion geometry. Testing was performed in the Icing Research Tunnel (IRT) at the NASA Glenn Research Center on a 36-inch chord NACA 0012 airfoil model. The goal of their study was to provide a better understanding of the variation in LWC, MVD, and temperature required to produce measurable changes in the geometry of an ice accretion. Miller et al.[2] tested at two freezing fractions, 0.3 and 0.7, and at airspeeds of 130 and 180 knots. The results of this study showed that parameter variations of less than 0.1 g/m^3 for LWC, 10μm for MVD, and 1ºF for temperature might generate distinct ice accretion geometry changes.

In 2006, Miller et al.[3] expanded upon their previous work by examining the effects of smaller variations in LWC and MVD. Unlike their previous study,[2] Miller et al.[3] did not directly control LWC and MVD variations. Instead, the spraybar air and water pressures were varied, which in turn controlled LWC and MVD variations. The nominal condition was defined by the following spraybar parameters, P_{air} = 25 psig, ΔP = 120 psid referenced to P_{air}, which corresponded to LWC and MVD of 0.827 g/m^3 and 28.7 μm, respectively. The spraybar pressures were varied around the baseline to produce an LWC range of 0.527 g/m^3 - 1.012 g/m^3, and an MVD range of 20.2 μm - 39.4 μm. Two freezing fractions, 0.39 and 0.75, were analyzed. It is important to note that these freezing fractions only correspond to the nominal spray bar condition and that the freezing fraction for off nominal conditions was slightly different. The results of this study showed that with a nominal freezing fraction of 0.39, a 15% increase in LWC from the nominal condition corresponded to a 0.08 inch increase in upper horn height and a 1.1 degree decrease in upper horn angle. At the same freezing fraction, a 15% increase in MVD corresponded to a 0.08 inch increase in upper horn height and a 2.3 degree decrease in upper horn angle. As a recommendation for future research, Miller et al.[3] proposed that aerodynamic performance (instead of ice accretion geometry) be used as a metric for evaluating the accuracy in LWC and MVD required for the simulation and measurement of simulated icing conditions. This provided motivation for the current study.

Bragg, Broeren, and Blumenthal[4] identified four ice accretion classifications based on iced-airfoil aerodynamics: ice roughness, streamwise ice, horn ice, and spanwise-ridge ice. Miller et al.[2,3] analyzed two of the classifications: streamwise ice and horn ice. Streamwise ice forms in colder conditions where the droplets freeze immediately on contact with the surface. In general, the geometry of a streamwise ice accretion starts at the leading edge and protrudes outward in the direction of the incoming flow. The streamwise ice accretions obtained by Miller et al.[3] had a nominal freezing fraction of 0.75. Horn ice is formed at warmer temperatures that are close to the freezing point. The geometry of horn ice is characterized by upper and lower surface ice protrusions that point away from the leading edge at some angle to the freestream. These protrusions, or ice horns, are formed because the droplets do not freeze immediately when they impinge on the airfoil or ice accretion. Instead, liquid water exists on the surface which can flow on the surface. Horns are formed as a result of this process. The horn ice accretions

obtained by Miller et al.[3] had a nominal freezing fraction of 0.39. In general, the geometry of horn ice can be quantified by the horn height and its location on the airfoil, whereas the geometry of streamwise ice is more difficult to simplify and was not analyzed in the current study.

In order to obtain the relationship between icing cloud parameters and iced airfoil performance, the sensitivity of iced airfoil performance to ice accretion geometry must be known. In general, airfoil performance decreases significantly with an ice accretion on the leading-edge. Papadakis et al.[5,6] studied the aerodynamic effects of simulated ice accretions on a NACA 0011 airfoil. The investigators used flat plates to simulate horn ice and showed that upper and lower surface horns with a normalized height (k/c) of 0.0625 reduced lift by as much as 150% (indicating C_l sign reversal) and increased drag by as much as 2000% from the clean airfoil. Additionally, they showed that simulated ice accretions with k/c = 0.125 reduced lift by a maximum of 200% and increased drag by a maximum of 4000% when compared to the clean airfoil.

In addition to height, the location of an ice accretion plays a key role in determining the magnitude of the aerodynamic performance loss. Kim and Bragg[7] investigated the effects of ice accretion geometry on airfoil performance by using simple geometric shape ice simulations on an NLF(1)-0414 airfoil. They showed that ice surface location and ice horn height both have an effect on airfoil performance degradation. Broeren et al.[8] investigated the effects of ice accretion and airfoil geometry on airfoil aerodynamic performance. They tested three different airfoil sections including the NACA 23012, NLF 0414, and NACA 3415 with three different types of ice accretions: supercooled large droplet ridge ice, glaze horn type ice, and intercycle ice. Like Kim and Bragg[7], they showed that horn height and surface location had the biggest impact on airfoil performance degradation. Additional details on the effects of horn ice on airfoil aerodynamic performance can be found in Bragg et al.[4]

The objective of this research was to use experimental data to determine the relationship and sensitivity of iced-airfoil performance to icing cloud parameter variations. This relationship expands upon previous work done by Miller et al.[2,3] regarding the required accuracy of LWC and MVD for simulating icing conditions. In addition, these data were placed in perspective by relating measurable or significant aircraft performance changes to the underlying changes in airfoil aerodynamic performance.

The approach for this research can be broken down into three parts: the ice accretion characteristics due to icing cloud parameters, the sensitivity of airfoil aerodynamic performance to ice accretion geometry, and the application of 2-D airfoil performance to aircraft performance. The first part of this research was extracted from the data of Miller et al.[3] Included in these data were ice accretion tracings that were modeled and installed on a NACA 0012 airfoil model for testing in the Illinois tunnel. The second part of this research was conducted in the Illinois tunnel, where sensitivities of C_{lmax}, C_{dmin}, and $(L/D)_{max}$ to ice accretion geometry were obtained. The third part of this research was done analytically. The sensitivity of stall speed (V_{stall}) to C_{lmax} was obtained for a model of a transport category turboprop airplane that was developed using equations and data found in References 9-11. The three previously mentioned sensitivities were then combined to form a sensitivity of aircraft performance to icing cloud parameters.

II. Experimental Methods

The experiments for this research were performed in the Illinois subsonic, low-turbulence, open-return wind tunnel. This wind tunnel is an open-return tunnel which exhausts into the tunnel room. The inlet contains a four-inch thick honeycomb flow straightener followed by four anti-turbulence screens, which reduce the empty test section turbulence intensity to less than 0.1% at all operating speeds.[12] The inlet to test section contraction ratio is 7.5:1. The test section is approximately 2.8 feet high, 4 feet wide, and 8 feet long and widened approximately 0.5 inch over the length to account for the growth in the boundary layer. The maximum rpm of the fan is 1200 rpm, which corresponds to a maximum empty test section speed of 160 mph.

Figure 1 is a diagram of the test section of the Illinois wind tunnel. Aerodynamic measurements were obtained with either a three-component force balance or a wake rake mounted behind the wind tunnel model. The force and moment balance was used for C_l and C_m, and the wake rake was used for C_d. The

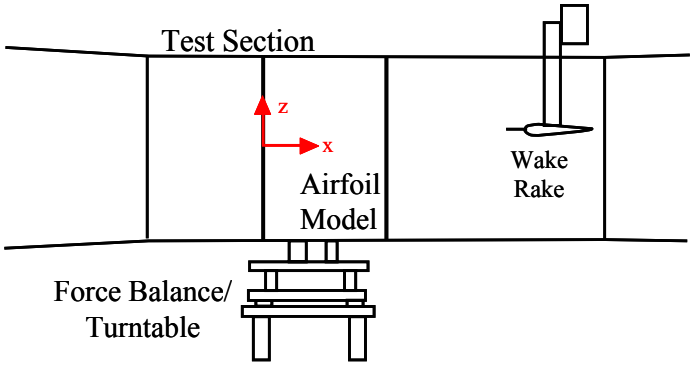

Figure 1. Schematic of the Illinois wind tunnel test section.

wind tunnel model was installed vertically in the test section.

Wind tunnel testing was conducted at a Reynolds number of 1.8 x 10^6, which corresponded to a Mach number of approximately 0.18. A computer directed two angle-of-attack sweeps, one in the positive direction and one in the negative direction, for each model configuration.

The airfoil model used in the Illinois 3x4 ft wind tunnel was an aluminum NACA 0012 airfoil with an 18-inch chord, 33.563-inch span, and a removable leading edge. The removable leading edge joined to the main body at 5% chord on the upper surface and 10% chord on the lower surface. The clean removable leading edge could be replaced with an alternate leading edge which contained a simulated ice accretion. For more information on the wind tunnel model refer to Gurbacki.[13]

The alternate leading edge attached to the main body of the airfoil in two half-span pieces, each 16.78 inches long. Figure 2 shows the cross-section of an alternate leading edge. In the picture, the left side of the part is where it mated to the airfoil model, and the right side of the part is the simulated ice accretion. The two half-span sections were sealed together using room temperature vulcanizing silicone (RTV) to prevent air from leaking between the sections. In addition, book tape was used to seal the upper and lower surface gaps between the alternate leading edge and the main body of the airfoil. The alternate leading edge was secured to the main body using six bolts that were fastened through the lower surface of the alternate leading edge. The bolt holes were filled with modeling clay to make a smooth contour with the model exterior.

Fig. 2. Cross-section of an alternate leading edge. Picture is showing one end of the simulated ice accretion, corresponding to IRT run 58.

The alternate leading edges were based on ice accretions produced in the NASA IRT by Miller et al.[3] These ice accretions were formed under different icing conditions, which resulted in geometry differences between the ice accretions. The method used by Miller et al.[3] to quantify the ice accretion geometry was to use the THICK program to record horn thickness and horn angle. Two freezing fractions were tested by Miller et al.[3] to capture the sensitivity of icing parameter variation on both streamwise ice and horn ice. As discussed in the introduction, the geometry of horn ice is more easily defined and thus was used in this study. Horn ice corresponded to a nominal freezing fraction of 0.39. The matrix of icing conditions tested by Miller et al.[3] and the resulting upper surface horn geometries are given in Table 1 for a nominal freezing fraction of 0.39.

Table 1. Test matrix of Miller et al.[3] for a nominal freezing fraction of 0.39. Ice horn geometry is for upper horn only.

Run	LWC g/m^3	MVD μm	Horn Height inches	Horn Angle degrees
19	0.985	38.9	2.28	128
20	0.955	36.7	2.37	133
21	0.925	34.6	2.34	138
22	0.893	32.6	2.33	141
23	0.861	30.6	2.22	144
24	0.827	28.7	2.21	145
25	0.791	26.9	2.05	145
26	0.629	20.2	1.60	162
27	0.674	21.8	1.58	156
28	0.715	23.5	2.01	155
29	0.754	25.2	1.81	151
42	0.827	28.7	2.24	151
43	0.753	21.3	1.92	160
44	0.888	23.1	2.13	149
45	0.825	23.9	2.15	157
46	0.979	26.5	2.42	146
47	0.892	26.7	2.26	149
49	0.827	28.7	2.32	141
50	0.628	25.1	1.84	149

Run	LWC g/m^3	MVD μm	Horn Height inches	Horn Angle degrees
51	0.672	27.5	2.10	149
52	0.714	29.9	2.25	139
53	0.753	32.4	2.43	143
54	0.753	21.3	2.03	156
55	0.825	23.9	2.28	147
56	0.892	26.7	2.40	138
57	0.954	29.6	2.41	141
58	1.012	32.9	2.39	129
59	0.888	23.1	2.23	148
60	0.979	26.5	2.45	140
61	0.912	21.6	2.26	149
62	0.999	24.4	2.57	142
78	0.625	35.5	2.19	164
83	0.527	28.2	1.72	152
84	0.578	31.8	1.86	145
85	0.669	39.4	2.21	140
133	0.827	28.7	2.15	141
134	0.827	28.7	2.36	144
135	0.827	28.7	2.50	143
136	0.827	28.7	2.41	141

For the current research, SMAGGICE[14] was used to quantify ice accretion geometry. SMAGGICE is less automated than other programs, which allowed more "engineering judgment" in the geometry determination. This is important because the arbitrariness of ice accretion geometry includes subtleties that are difficult to classify and are better identified without automation. The ice accretions were measured in terms of normalized horn height (k/c) and normalized horn position (s/c). Figure 3 shows how SMAGGICE represents ice accretion geometry.

Each ice accretion had unique values of k/c and s/c that corresponded to the LWC and MVD at which it was formed. It should be noted that the lower surface horn was assumed to have very little effect on C_{lmax}. This assumption was based on work by Kim.[15] These data were compiled for a set of ice accretions to obtain a sensitivity of ice accretion geometry to icing cloud parameters. The results of this sensitivity were compared with an existing sensitivity of C_{lmax} to ice accretion geometry.[8] This comparison created an approximate relationship between C_{lmax}, LWC, and MVD. Out of the 39 runs conducted by Miller et al.[3], 11 were selected to be modeled and tested in the Illinois wind tunnel. One of the criteria for selection was the 11 selected ice accretions needed to cover a similar range of LWC and MVD as was covered by Miller et al.[3] Secondly, the selected ice accretions needed to capture the trends of C_{lmax}, as shown by the approximate relationship between C_{lmax}, LWC, and MVD. Table 2 shows the selected runs and the corresponding upper surface ice accretion geometries calculated using SMAGGICE. Figures 4 and 5 are contour plots showing the relationship between upper surface k/c and s/c to LWC and MVD. Figure 6 shows the geometry of ice accretions formed in the IRT at constant air pressure.

Table 2. Test matrix of selected ice accretions. Geometries were obtained with the SMAGGICE computer program for the upper surface horn.

Run	LWC g/m^3	MVD µm	k/c	s/c
19	0.985	38.9	0.0637	0.01450
21	0.925	34.6	0.0647	0.01282
49	0.827	28.7	0.0614	0.00845
26	0.629	20.2	0.0454	0.00216
29	0.754	25.2	0.0510	0.00767
46	0.979	26.5	0.0674	0.00907
51	0.672	27.5	0.0584	0.00767
58	1.012	32.9	0.0665	0.01450
61	0.912	21.6	0.0629	0.00767
83	0.527	28.2	0.0479	0.00588
85	0.669	39.4	0.0612	0.01020

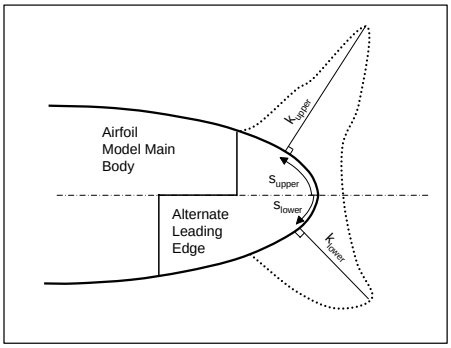

Fig. 3. SMAGGICE representation of typical horn ice accretion geometry.

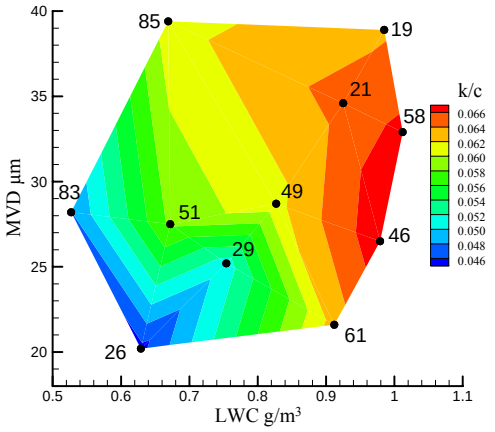

Fig. 4. Relationship of k/c to LWC and MVD.

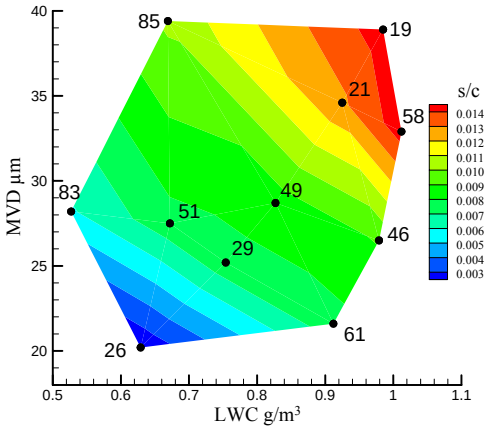

Fig. 5. Relationship of s/c to LWC and MVD.

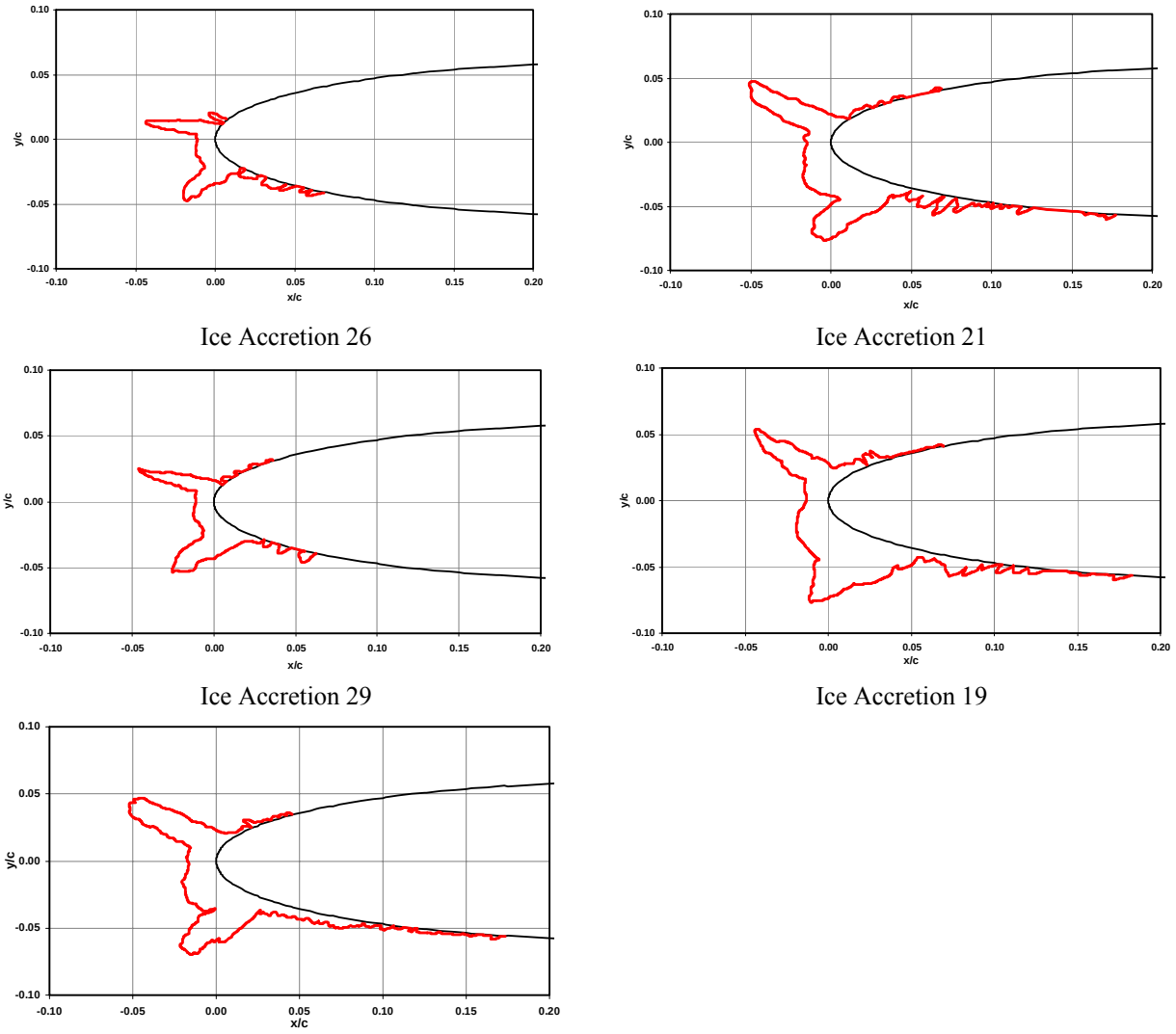

Fig. 6. Ice tracings of accretions formed in the IRT at constant P_{air} = 25 psig.

III. Results and Discussion

This section presents the clean model test results, followed by the iced airfoil results and comparisons to previous work. The effects of icing cloud parameter variations on iced airfoil performance as well as on aircraft performance are presented last.

Clean Model Results

Validation of the wind tunnel model was done by comparing the clean C_l, C_d, and C_m of this test with values from previous tests in the Illinois wind tunnel that used the same wind tunnel model. This validation was run at a Reynolds number of 1.8 x 10^6, which corresponded to a Mach number of 0.18. Figures 7, 8, and 9 show the results of the validation for lift, pitching moment, and drag, respectively.

In the cases of lift and pitching moment coefficient, the data matched almost exactly. Both tests found the clean C_{lmax} to be roughly 1.35. In addition, the drag polar data compared well except for a single data point located at C_l = 0.8, and for a few data points near C_{dmin}. The single data point difference was repeatable throughout the duration of the current test. Near C_{dmin}, the maximum wake drag variation between tests was 20 counts.

This is a relatively small variation in drag which could be the result of surface imperfections on the model. Overall, the magnitude of test-to-test drag variation was considered to be negligible compared to the expected drag increments due to the simulated ice accretions.

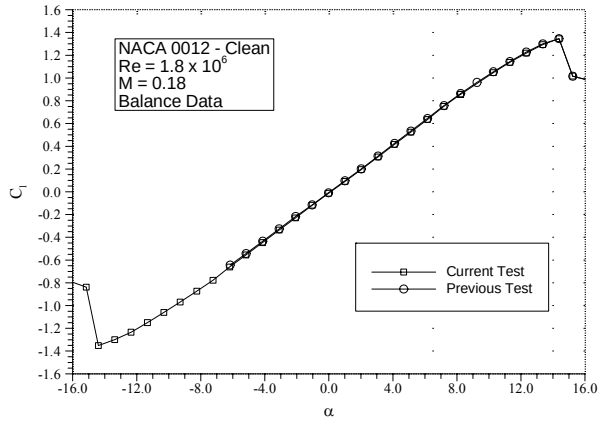

Fig. 7. Test-to-test lift coefficient repeatability.

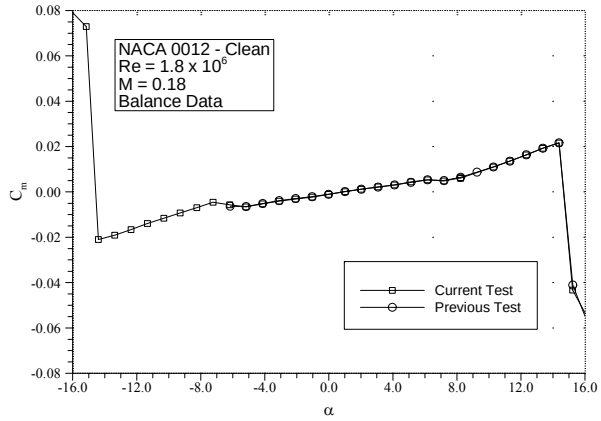

Fig. 8. Test-to-test pitching moment coefficient repeatability.

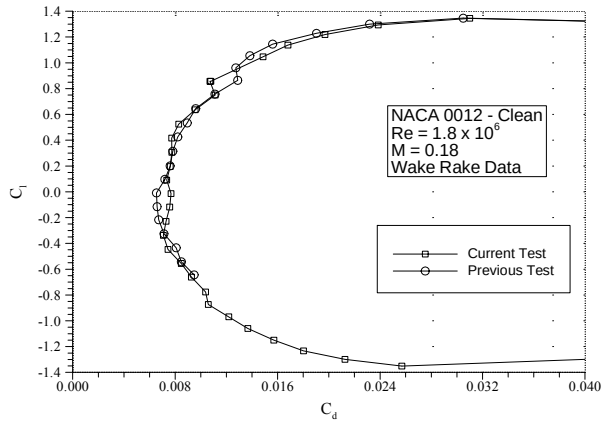

Fig. 9. Test-to-test drag polar repeatability.

was the angle-of-attack at which the ice accretions were formed.

Iced Airfoil Aerodynamics

For this study, eleven simulated ice accretions were tested. Each simulated ice accretion was two dimensional, meaning there was no geometry variation in the spanwise direction. In general, each ice accretion was tested at a Reynolds number of 1.8 x 10^6. Positive and negative angle of attack sweeps were performed until stall, where C_{lmax} was defined as the first local maximum or minimum of C_l vs. α. Each simulated ice accretion was labeled to correspond to its IRT run number obtained from Miller et al.[3] For more information on the ice accretions refer to Campbell.[17]

Generally speaking, all simulated ice accretions significantly affected the aerodynamics of the model. Figure 10 is a contour plot showing the relationship between the maximum lift coefficient and upper surface horn k/c and s/c. The effect of the lower horn on C_{lmax} was considered very small based on the results of Kim.[15] The maximum lift coefficient of the clean model was deceased by the range of 0.73 to 1.15 with alternate leading-edges attached. These increments corresponded to a 50% to 80% reduction in C_{lmax}, respectively. Interestingly, Fig. 10 shows that percent change in s/c corresponds to a larger change in C_{lmax} than a percent change in k/c. Additionally, the stall behavior of the iced configurations indicated that the addition of simulated ice shapes to the airfoil changed the stall type from leading-edge stall to thin airfoil stall. This behavior is apparent in Fig. 11, which compares the lift curves for the set of ice accretions formed under constant spraybar air pressure, P_{air} = 25 psig. Refer to Fig. 6 for the geometry of these ice accretions.

Figure 12 presents the pitching moment curves for the set of ice accretions formed under constant spraybar air pressure, P_{air} = 25 psig. The pitching moment exhibited a roughly linear positive slope with angle-of-attack ($C_{m\alpha} > 0$) in the non-stalled region for the clean configuration. However, with simulated ice accretions attached, the pitching moment was more sensitive to angle-of-attack changes, and in the case of the larger ice accretions (19, 21, 49), $C_{m\alpha}$ actually became negative. Another observation was that the iced configuration pitching moment curves all intersected at approximately 2.5 degrees, which

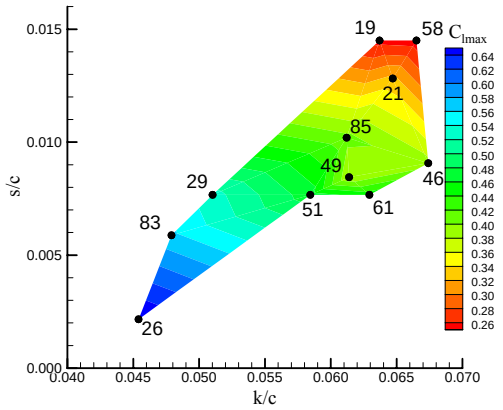

Fig. 10. Contour plot showing the relationship of C_{lmax} to upper horn k/c and s/c.

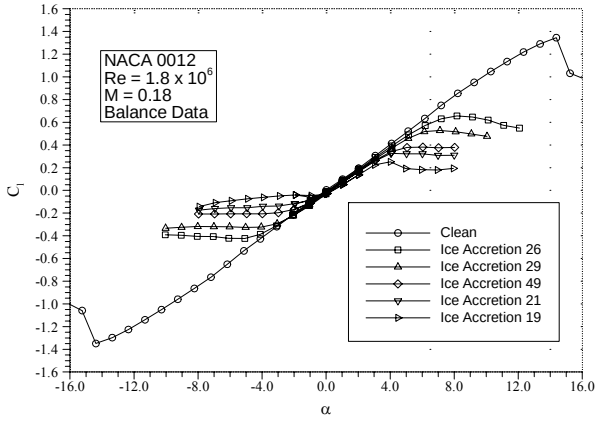

Fig. 11. Lift curves of a selected set of ice accretions formed under constant spraybar air pressure.

Figure 13 compares the drag polars of the set of ice accretions formed under constant spraybar air pressure, P_{air} = 25 psig. The minimum drag of the simulated ice accretions was 400% to 2000% above the value for the clean model. The C_l corresponding to C_{dmin} was approximately 0.1 for all iced configurations. Interestingly, this C_l corresponded to an angle-of-attack of about 1 degree, which was 1.5 degrees below the angle-of-attack at which the ice accretions were formed. Furthermore, it was observed that the iced configuration drag polars were much more sensitive to angle-of-attack changes than for the clean configuration. This affected the maximum lift to drag ratios of the iced airfoils, which were reduced by 88% to 98% from the clean configuration.

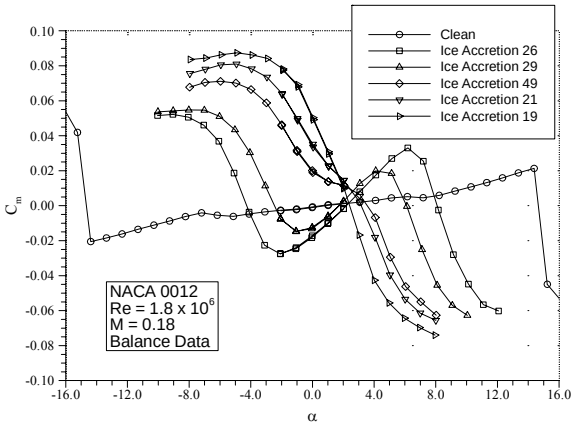

Fig. 12. Pitching moment curves of a selected set of ice accretions formed under constant spraybar air pressure.

Although Kim[15] showed that C_{lmax} is primarily a function of the upper horn geometry, C_{dmin} and $(L/D)_{max}$ have been shown to be a function of the lower horn geometry as well. Olsen et al.[16] illustrated the dependence of drag on icing conditions, and in turn ice accretion geometry. Figures 14 and 15 show C_{dmin} as a function of upper horn and lower horn geometry, respectively. Both figures show a similar trend; C_{dmin} increases with increasing upper and lower surface horn k/c and s/c. Figures 16 and 17 display $(L/D)_{max}$ as a function of upper horn and lower horn geometry, respectively. Similar to the plots of C_{dmin}, Figs. 16 and 17 show $(L/D)_{max}$ to decrease with increasing k/c and s/c. It was shown that both the upper and lower surface horns have an effect on C_{dmin} and $(L/D)_{max}$, but the effect of each horn could not be isolated. Therefore, it can be said that the upper and lower surface horns both are affected by changes in the icing conditions and they both decrease airfoil performance with increasing horn height and location. However, the upper and lower geometries are not independent and cannot be simplified further due to the controlled set of experimental accretions used in this study.

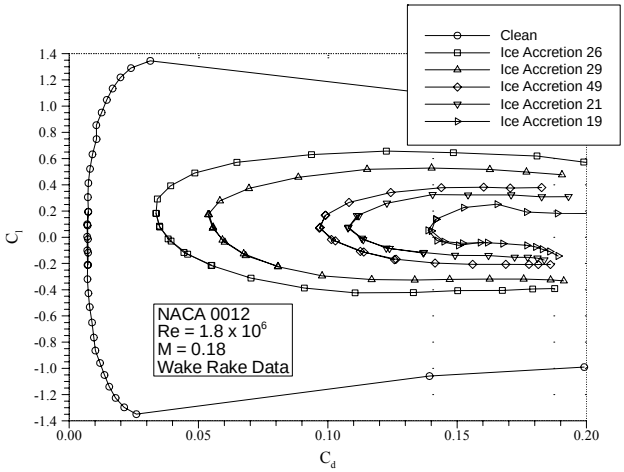

Fig. 13. Drag polars of selected set of ice accretions formed under constant spraybar air pressure.

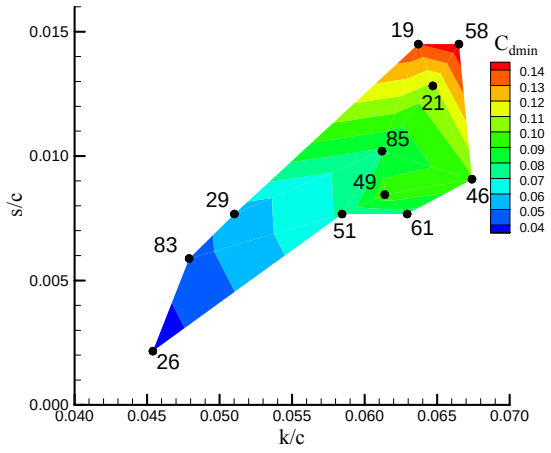

Fig. 14. Contour plot showing the relationship of C_{dmin} to upper horn k/c and s/c.

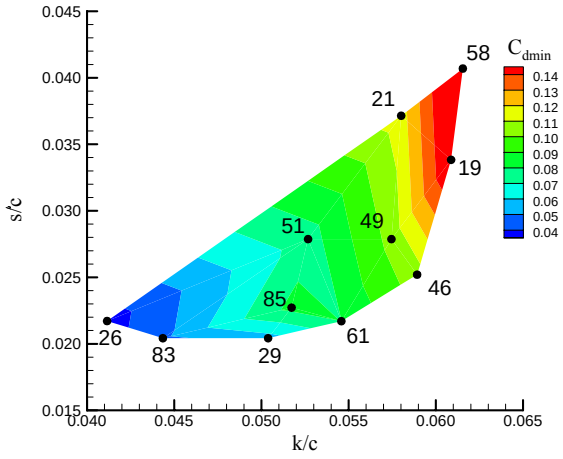

Fig. 15. Contour plot showing the relationship of C_{dmin} to lower horn k/c and s/c.

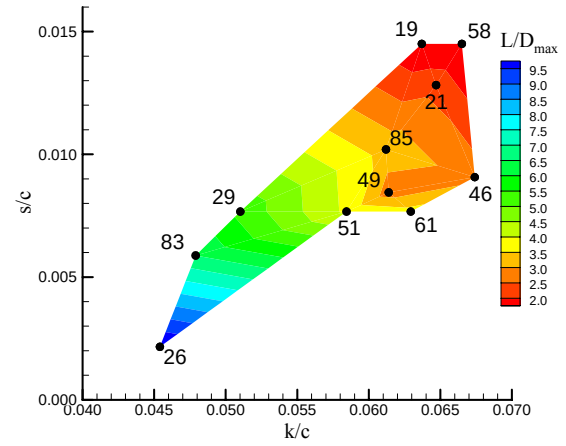

Fig. 16. Contour plot showing the relationship of L/D_{max} to upper horn k/c and s/c.

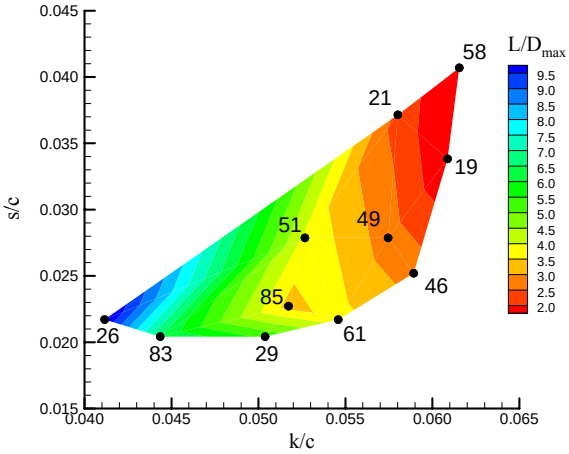

Fig. 17. Contour plot showing the relationship of L/D_{max} to lower horn k/c and s/c.

The sensitivity of airfoil performance to ice accretion geometry obtained with this research was compared to a similar study conducted by Broeren et al.[8] Broeren et al.[8] used simple geometric shapes to simulate ice accretions on a NACA 23012 airfoil model, then investigated the effect of the simple geometric shape geometry on the aerodynamics. Broeren et al.[8] conducted their study in the Illinois subsonic wind tunnel, where they used the same Reynolds number and model scale as the current research. However, Broeren et al.[8] only analyzed the effects of an upper surface ice horn, whereas the current research investigated the effects of upper and lower surface ice horns. The other significant difference between the current research and Broeren et al.[8] is a difference in baseline airfoil models (NACA 0012 used in this research and NACA 23012 used by Broeren et al.[8]).

Because the current research and Broeren et al.[8] used different airfoil models the change in C_{lmax} from the clean configuration was compared. Selected results of Broeren et al.[8] were reformatted as a contour plot and are shown in Fig. 18. For the current research, the relationship between C_{lmax}, k/c, and s/c was plotted as percentage change from the clean configuration in Fig. 19.

A comparison of Figs. 18 and 19 shows similar trends between this study and Broeren et al.[8] However, for the range of k/c and s/c tested in the current research, the percent decrease of C_{lmax} found by Broeren et al.[8] was observed to be significantly less. In the current research, the percentage decrease in C_{lmax} from the clean configuration ranged from 50% to 80%, whereas over a comparable range of k/c and s/c, the data of Broeren et al.[8]

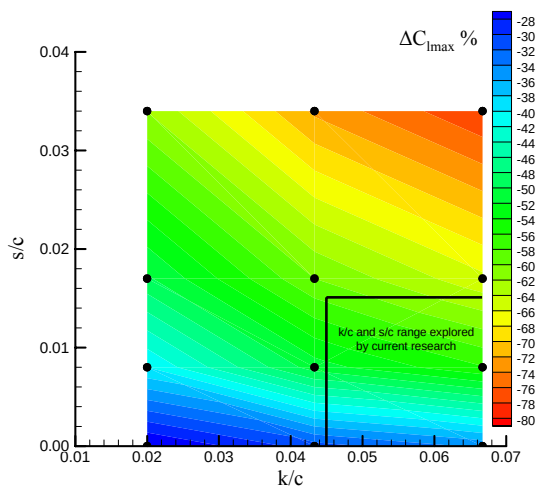

Fig. 18. Data of Broeren et al.[8] showing percent decrease in C_{lmax} from the clean configuration due to upper surface horn geometry on a NACA 23012 airfoil model.

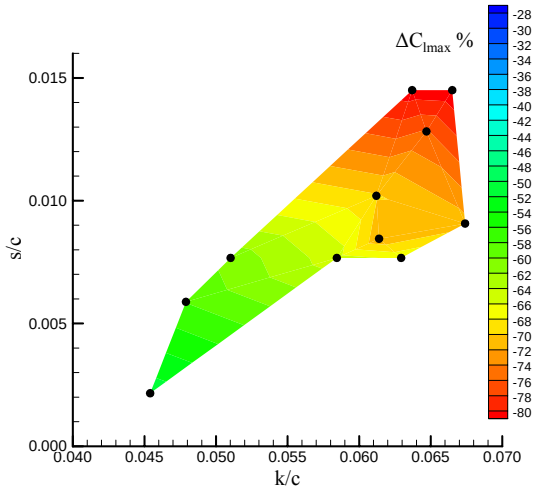

Fig. 19. Percent decrease in C_{lmax} from the clean configuration using upper horn data from the current research on a NACA 0012 airfoil model.

showed a decrease in C_{lmax} of 30% to 60%. Therefore, the decrease in C_{lmax} from the clean configuration as observed by the current research was found to be roughly 20% more than the data produced by Broeren et al.[8] A reason for the difference could be a result of different airfoil sections between the studies. Another reason could be that Broeren et al.[8] only tested an upper ice horn, whereas both upper and lower surface ice horns were tested in the current research. The latter reason is less likely because Kim[15] found the effect of the lower horn to be negligible in the determination of C_{lmax}.

Sensitivity of Iced Airfoil Performance to Changes in Icing Parameters

The results of the current research were combined with data obtained from Miller et al.[3] to form a sensitivity of airfoil aerodynamic performance to icing cloud conditions. The baseline ice accretion was number 49, which corresponded to the baseline conditions of LWC = 0.827 g/m^3 and MVD = 28.7 μm as set by Miller et al.[3] The change in LWC and MVD from the baseline condition were calculated for each ice accretion, followed by the corresponding change in airfoil performance. Table 3 shows the results of this procedure as a sensitivity of airfoil performance to icing cloud conditions. The following parameters were held constant for the formation of the ice accretions: t = 15 min, V = 200 knots, α = 2.5 degrees, T_{tot} = 23 degrees F, and T_s = 13.5 degrees F. Also, the baseline freezing fraction was 0.39, but varied at off-baseline conditions.

Table 3. Sensitivity of airfoil performance to icing cloud parameters. Note that Δ is the change from the ice accretion 49 baseline condition. (t = 15 min, V = 200 knots, α = 2.5°, T_{tot} = 23°F, T_s = 13.5°F, $\eta_0 \approx 0.39$)

Accretion	LWC g/m^3	MVD μm	C_{lmax}	C_{dmin}	$(L/D)_{max}$	ΔLWC g/m^3	ΔMVD μm	ΔC_{lmax}	ΔC_{dmin}	$\Delta(L/D)_{max}$
clean	N/A	N/A	1.345	0.0071	81.44	N/A	N/A	N/A	N/A	N/A
19	0.985	38.9	0.252	0.1400	1.52	0.158	10.2	-0.130	0.0432	-1.22
21	0.925	34.6	0.326	0.1078	2.32	0.098	5.9	-0.056	0.0110	-0.42
26	0.629	20.2	0.662	0.0336	10.08	-0.198	-8.5	0.280	-0.0632	7.34
29	0.754	25.2	0.528	0.0537	5.36	-0.073	-3.5	0.146	-0.0431	2.62
46	0.979	26.5	0.387	0.0990	2.78	0.152	-2.2	0.005	0.0022	0.04
49 baseline	0.827	28.7	0.382	0.0968	2.74	0.000	0.0	0.000	0.0000	0.00
51	0.672	27.5	0.469	0.0714	3.90	-0.155	-1.2	0.087	-0.0254	1.16
58	1.012	32.9	0.248	0.1487	1.45	0.185	4.2	-0.134	0.0519	-1.29
61	0.912	21.6	0.451	0.0757	3.69	0.085	-7.1	0.069	-0.0211	0.95
83	0.527	28.2	0.564	0.0458	6.50	-0.3	-0.5	0.182	-0.0510	3.76
85	0.669	39.4	0.406	0.0784	3.30	-0.158	10.7	0.024	-0.0184	0.56

Table 3 includes absolute values of maximum lift coefficient, minimum drag coefficient, and maximum lift to drag ratio, as well as their changes from the baseline condition. Refer to Campbell[17] for more information on the selected ice accretions.

Figure 20 shows the change in C_{lmax} from the run 49 baseline condition as a function of ΔLWC and ΔMVD. Boxes were drawn around the baseline condition to indicate 10% and 15% variation in LWC and MVD. Of the set of ice accretions tested, the maximum variation in C_{lmax} was 0.28, which occurred at ΔLWC = -0.198 g/m^3 and ΔMVD = -8.5 µm. Inside the 10% box, the maximum variation in C_{lmax} was 0.12 and in the 15% box it was 0.18.

In general, a decrease in LWC and MVD had a stronger effect on ΔC_{lmax} than an increase in LWC and MVD. This could be a result of the already large size of the baseline ice accretion. In other words, the baseline ice accretion performance was closer to the lower bound of C_{lmax} than the upper bound, so any increase in ice accretion size would have less of an effect than if the baseline ice accretions were smaller. Figure 21 shows ΔC_{dmin} as a function of ΔLWC and ΔMVD. The maximum variation of C_{dmin} over the set of ice accretions was -0.0681, which occurred at ΔLWC = -0.198 g/m^3 and ΔMVD = -8.5 µm. The maximum variation of C_{dmin} inside the 15% box was -0.05, and inside the 10% box it was -0.03. Figure 22 shows the effect of ΔLWC and ΔMVD on $\Delta(L/D)_{max}$. The maximum variation in $\Delta(L/D)_{max}$ occurred at ΔLWC = -0.198 g/m^3 and ΔMVD = -8.5 µm and was equal to 7.34. Inside the 15% box the maximum variation was 4 and inside the 10% box the maximum variation was 2. In general, airfoil performance decreased with increasing LWC and MVD. This was expected because larger LWC and MVD corresponded to larger ice accretions. Over the range of icing conditions tested, it appeared that a percentage change in LWC had a slightly larger effect than an equivalent change in MVD. In explanation, LWC is a measure of how much water is in the icing cloud surrounding the airfoil and MVD determines, in part, how much of that water impinges on the airfoil. Because the ice accretions studied in this research had a large frontal area, and the MVD was relatively large, the effect of MVD was somewhat mitigated. This trend was also seen in the data of Miller et al.[3] which showed that LWC and MVD had about an equal effect on s/c of the horn, but LWC had a stronger effect on k/c. Refer to Figs. 4 and 5 for a graphical representation of the effects of LWC and MVD on ice accretion geometry.

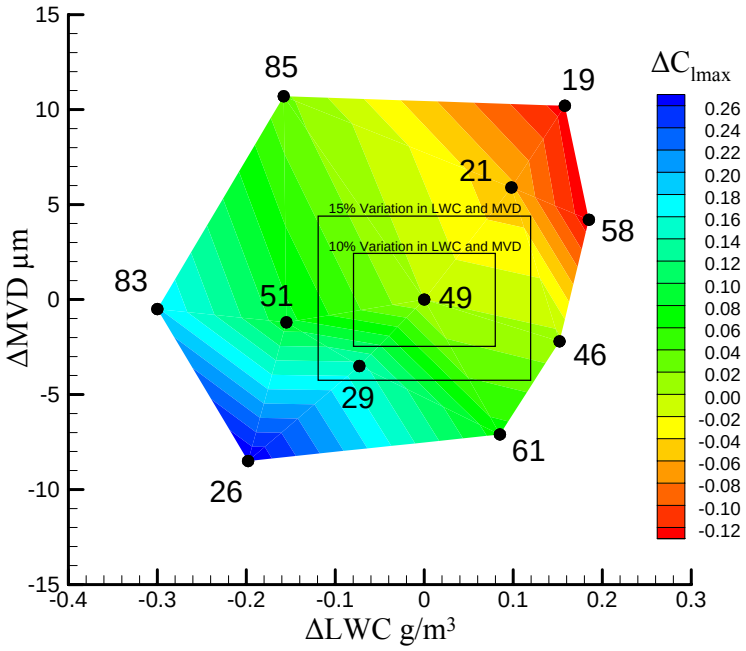

Fig. 20. Effect of icing cloud parameter variations on C_{lmax}. NACA 0012, Re = 1.8 x 10^6, M = 0.18. Numbers correspond to IRT run number and are described in Table 2.

A different perspective on these data can be obtained by analyzing the ΔLWC and ΔMVD corresponding to a measurable or significant change in C_{lmax}. A measurable change in C_{lmax} was considered to be the aerodynamic uncertainty calculated by Campbell.[17] The uncertainty in C_l at the stalling angle-of-attack for the airfoil which contained the baseline ice accretion was approximately 0.001. Figure 20 was interpolated and showed that this uncertainty in C_{lmax} corresponded to a ΔLWC of ±0.004 g/m^3 assuming ΔMVD = 0, or a ΔMVD of ±0.2 µm assuming ΔLWC = 0. These are the minimum values of ΔLWC and ΔMVD that would produce a change in C_{lmax} as determined by the aerodynamic wind tunnel uncertainty in C_l. This interpolation was performed about the baseline condition along lines of zero ΔLWC or ΔMVD. In general, the ΔLWC and ΔMVD resulting from an increase in C_{lmax} were different than the ΔLWC and ΔMVD resulting from a decrease in C_{lmax}. The two results were averaged to get an effective change in LWC and MVD. Therefore it should be noted that this sensitivity is unique to the

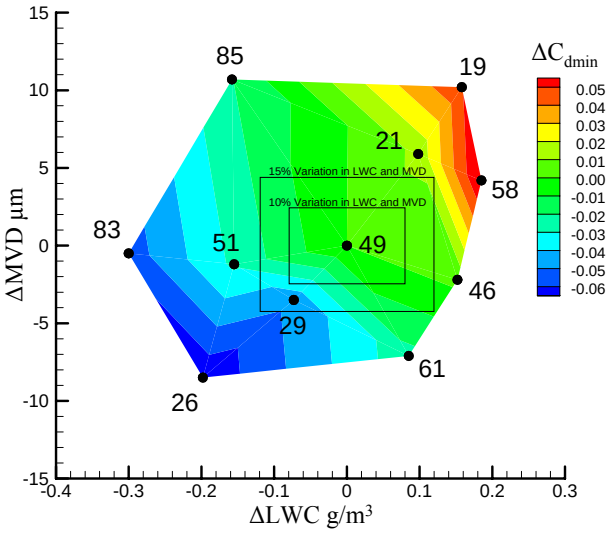

Fig. 21. Effect of icing cloud parameter variations on C_{dmin}. NACA 0012, Re = 1.8 x 10^6, M = 0.18. Numbers correspond to IRT run number and are described in Table 2.

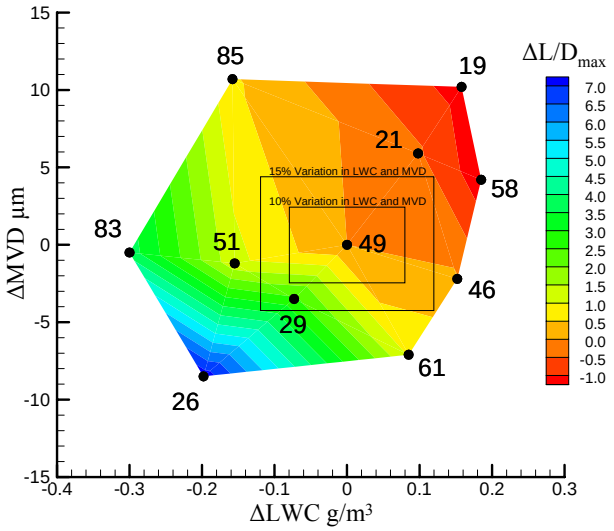

Fig. 22. Effect of icing cloud parameter variations on $(L/D)_{max}$. NACA 0012, Re = 1.8 x 10^6, M = 0.18. Numbers correspond to IRT run number and are described in Table 2.

baseline point (run 49, LWC = 0.827 g/m^3, MVD = 28.7 µm). This process was applied to ΔC_{dmin} in the same way as it was applied to ΔC_{lmax}. The uncertainty in C_{dmin} was calculated to be approximately 0.0005 for an airfoil containing the baseline ice accretion. Interpolating Fig. 21 shows that the uncertainty in C_{dmin} corresponds to a ΔLWC of ±0.006 g/m^3 assuming ΔMVD = 0, or a ΔMVD of ±0.3 µm assuming ΔLWC = 0. This analysis effectively shows that the ΔLWC and ΔMVD required to discern changes in airfoil performance on the order of the aerodynamic wind tunnel uncertainty are extremely small.

A significant change in C_{lmax} was defined for the purpose of this research as the ΔC_{lmax} corresponding to the difference between 2-D and 3-D simulated ice accretions. Gurbacki[13] found that a NACA 0012 with a 3-D casting simulated ice accretion had a C_{lmax} 0.03 greater than a NACA 0012 with a 2-D smooth simulated ice accretion. This accuracy of ΔC_{lmax} = 0.03 then represents, at least for Gurbacki's[13] test, the accuracy with which an ice accretion can be simulated for aerodynamic testing. Using the same interpolation scheme as before, the ΔLWC and ΔMVD corresponding to this change in C_{lmax} were ±0.11 g/m^3 and ±4.6 µm, respectively. These data were equal to a 13.3% change in LWC and a 16.0% change in MVD from the baseline condition. The ΔC_{dmin} found by Gurbacki[13] was 0.0058. This corresponded to a 7.3% change in LWC and a 10.8% change in MVD from the baseline condition. Table 4 presents the accuracy required in ΔLWC and ΔMVD to simulate measurable and significant values of ΔC_{lmax} about the baseline point.

Table 4. Required accuracy of ΔLWC and ΔMVD based on iced-airfoil performance at the baseline condition (LWC = 0.827 g/m^3, MVD = 28.7 µm, Ice accretion 49).

Change in airfoil performance	Qualitative significance	ΔLWC	ΔMVD	ΔLWC (% from baseline)	ΔMVD (% from baseline)
ΔC_{lmax} = ±0.001	Aerodynamic wind tunnel uncertainty	±0.004 g/m^3	±0.2 µm	0.5%	0.7%
ΔC_{dmin} = ±0.0005	Aerodynamic wind tunnel uncertainty	±0.006 g/m^3	±0.3 µm	0.7%	1.0%
ΔC_{lmax} = ±0.03	Change in C_{lmax} between 2D and 3D ice accretions	±0.11 g/m^3	±4.6 µm	13.3%	16.0%
ΔC_{dmin} = ±0.0058	Change in C_{dmin} between 2D and 3D ice accretions	±0.06 g/m^3	±3.1 µm	7.3%	10.8%

Sensitivity of Aircraft Performance to Changes in Icing Parameters

Another approach to assessing the required accuracy in LWC and MVD is finding the ΔLWC and ΔMVD corresponding to measurable or significant changes in aircraft performance. One important performance metric is stall speed, which can be related to C_{lmax} and then to ΔLWC and ΔMVD. A generic model of a turboprop transport aircraft was developed. It is important to note that due to the complexities involved in the modeling of full aircraft

performance based solely on two dimensional data, this sensitivity should be treated only as a first step in the extension of this research. To achieve better results, 3-D testing should be performed.

The objective of this aircraft model was to produce representative stall speeds and sensitivities for a given lift curve and aircraft parameters. Table 5 gives the aircraft model parameters used for the current research.

Table 5. Aircraft model parameters.[9]

Aircraft Weight	25,000 lbs
Altitude	10,000 feet
Planform Area	450 ft^2
Clean C_{Lmax}	1.7

The sensitivity of stall speed to icing cloud parameter variations was obtained by first finding the change in airfoil section C_{lmax} from the clean configuration for each iced configuration, and then Eqs. 1 and 2 were used to approximate the iced C_{Lmax} for the aircraft model.

$$\Delta C_{L_{\max}} = \frac{S_{iced}}{S} \cdot \Delta C_{l_{\max}} \tag{1}$$

$$C_{L_{\max,ice}} = C_{L_{\max,clean}} + \Delta C_{L_{\max}} \tag{2}$$

The parameter S is the planform area of the wing and S_{iced} is the total planform area behind a leading-edge ice accretion. Equation 1 is a modification of a method in Raymer[11] which was intended to estimate the 3-D C_{Lmax} increment from 2-D data for the deployment of partial span flaps. In the modified equation, the ratio of S_{iced} to S was determined to be 0.83 by calculating the ratio of C_{Lmax} of an aircraft containing a simulated wing ice accretion to the 2-D C_{lmax} of wind tunnel data with a comparable simulated ice accretion. The data for this comparison was obtained from icing flight test data and 2-D wind tunnel data with similar ice accretions.[17,18] The value of the ratio of S_{iced} to S seemed reasonable based on ratios of exposed planform area to total planform area for typical transport category turboprop aircraft. Stall speed was calculated with Eq. 3

$$V_{stall} = \sqrt{\frac{2 \cdot W}{\rho \cdot C_{L_{\max}} \cdot S}} \tag{3}$$

where W is the aircraft weight and ρ is air density.[9] The change in stall speed resulting from an ice accretion was computed with Eq. 4.

$$\Delta V_{stall} = V_{stall,iced} - V_{stall} \tag{4}$$

The sensitivity of stall speed to icing cloud parameter variations was calculated using the previously discussed procedure. The aircraft was assumed to be a transport category turboprop, flying at 10,000 feet with a weight of 25,000 lbs. These conditions were chosen because 25,000 lbs is a typical operating weight for this type of turboprop, and a review of the NTSB accident database revealed that 10,000 feet is a common altitude to experience icing conditions. The sensitivity of stall speed to LWC and MVD variations is presented in Fig. 23. The clean stall speed was calculated to be 114 knots, and the baseline iced-aircraft stall speed was calculated to be 161 knots. Boxes were drawn around the baseline condition to indicate 10% and 15% variation in LWC and MVD. Of the set of ice accretions tested, the maximum variation in V_{stall} was -15.7 knots, which occurred at ΔLWC = -0.198 g/m^3 and ΔMVD = -8.5 μm. Inside the 10% box, the maximum variation in V_{stall} was approximately -7 knots and in the 15% box it was -9 knots.

To put these values into perspective, 16.1 knots corresponds to a 10% change from the stall speed of the aircraft containing the baseline ice accretion. Analogous to observations of the effect of k/c and s/c on C_{lmax}, a decrease in LWC and MVD had a stronger effect on V_{stall} than an increase in LWC and MVD. This is most likely a result of the

large size of the simulated ice accretions, which resulted in C_{lmax} being more sensitive to a decrease in ice accretion size than an increase in ice accretion size.

In a similar fashion as the last section, the variation of LWC and MVD required to produce significant changes in aircraft performance were analyzed. Significant values of stall speed were found in FAA Advisory Circular AC-25-7A,[19] which is titled "Flight Test Guide for Certification of Transport Category Airplanes." According to AC-25-7A, stall speed is required to be known within 0.5 knots for the certification of transport airplanes. Additionally, if the ice accretions are shown to increase stall speed by 3 knots or greater, the reference airspeeds for that aircraft are required to be recalculated. This research investigated the variation of LWC and MVD required to generate these changes in stall speed. For $\Delta V_{stall} = \pm 0.5$ knots, Fig. 23 was interpolated to give $\Delta LWC = \pm 0.025$ g/m^3 assuming $\Delta MVD = 0$, and $\Delta MVD = \pm 1.1$ µm assuming $\Delta LWC = 0$. By the same procedure, if $\Delta V_{stall} = \pm 3$ knots, $\Delta LWC = \pm 0.12$ g/m^3, and $\Delta MVD = \pm 5.5$ µm. Table 6 presents the accuracy of LWC and MVD required to simulate measurable and significant values of ΔV_{stall}.

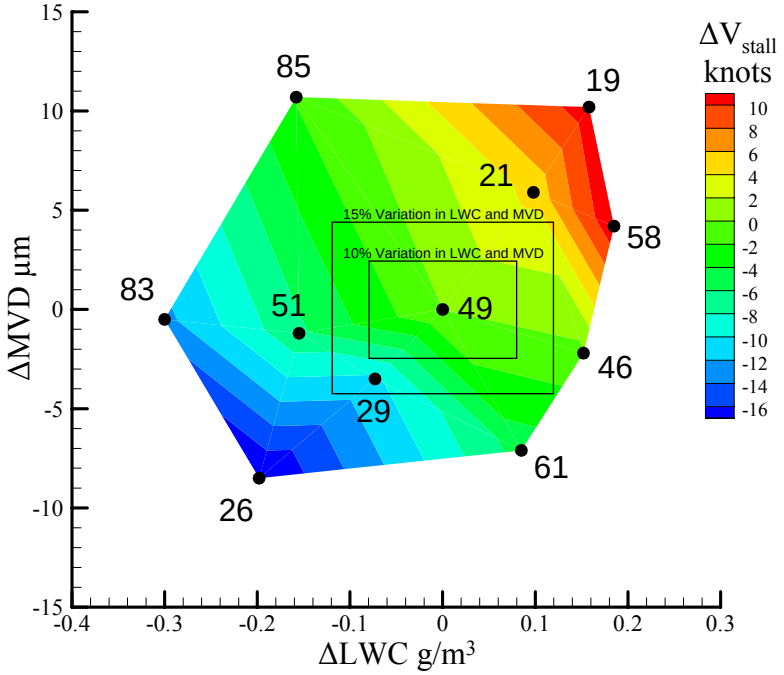

Fig. 23. Effect of icing cloud parameter variations on V_{stall} from the case 49 baseline. Numbers correspond to IRT run number and are described in Table 2.

Table 6. Required accuracy of ΔLWC and ΔMVD based on iced-aircraft performance at the baseline condition (LWC = 0.827 g/m^3, MVD = 28.7 µm, Ice accretion 49).

Change in aircraft performance	Qualitative significance	ΔLWC	ΔMVD	ΔLWC (% from baseline)	ΔMVD (% from baseline)
$\Delta V_{stall} = \pm 0.5$ knots	Stall speed must be known within 0.5 knots	±0.025 g/m^3	±1.1 µm	3.0%	3.8%
$\Delta V_{stall} = \pm 3$ knots	If $\Delta V_{stall} > 3$ knots due to ice, reference airspeeds need to be recalculated	±0.12 g/m^3	±5.5 µm	14.5%	19.2%

A comparison of the required accuracy in LWC and MVD for $\Delta V_{stall} = \pm 3$ knots and $\Delta C_{lmax} = \pm 0.03$ showed that the results were similar. Therefore one answer to the question of "how good is good enough?" might be LWC accuracy within 0.12 g/m^3 and MVD accuracy within 5.5 µm. However, it should be stated again that this sensitivity is only valid about the baseline ice accretion, 49, and baseline condition of LWC = 0.827 g/m^3 and MVD = 28.7 µm.

To expand the scale of this research, sensitivities of V_{stall} to LWC and MVD at off-baseline conditions were investigated. The off-baseline conditions were picked to correspond to ice accretions 21, 29, and 51 because they lie in the interior of Fig. 23. The ΔLWC and ΔMVD required for a change in stall speed of ±3 knots were calculated for each of these ice accretions at their respective ΔLWC and ΔMVD locations. Refer to Fig. 2.8 for tracing of these ice accretions. For ice accretion 29, which is a smaller accretion than the baseline accretion, a $\Delta V_{stall} = \pm 3$ knots corresponded to a change in LWC of ±0.1 g/m^3 and a change in MVD of ±3.5 µm. For ice accretion 21, a larger ice accretion than the baseline accretion, a $\Delta V_{stall} = \pm 3$ knots corresponded to a change in LWC of ±0.06 g/m^3 and a change in MVD of ±2.6 µm. For ice accretion 51, which is slightly smaller than the baseline ice accretion, a $\Delta V_{stall} = \pm 3$ knots corresponded to a change in LWC of ±0.07 g/m^3 and a change in MVD of ±4.9 µm. Table 7 compares

the baseline sensitivity to the sensitivities found for the off-baseline conditions. It was shown that the sensitivity of V_{stall} to LWC and MVD variations was dependent on which icing cloud parameters and ice accretion geometry were chosen to be baseline. However, in order to get a better sense of the trends associated with this dependence, either wider variations in LWC and MVD need to be explored, or the resolution of points in the current range of LWC and MVD need to be increased.

Table 7. Comparison of the off-baseline and baseline sensitivities of V_{stall} to LWC and MVD variations.

Ice Accretion	ΔV_{stall} knots	ΔLWC g/m^3	ΔMVD µm
49 (baseline) LWC=0.827 g/m^3, MVD=28.7 µm	±3	±0.12	±5.5
21 (off-baseline) LWC=0.925 g/m^3, MVD=34.6 µm	±3	±0.06	±2.6
29 (off-baseline) LWC=0.629 g/m^3, MVD=20.2 µm	±3	±0.10	±3.5
51 (off-baseline) LWC=0.672 g/m^3, MVD=27.5 µm	±3	±0.07	±4.9

IV. Summary and Conclusion

The objective of this study was to provide insight into the required accuracy of simulated icing conditions. An existing ice shape sensitivity to icing cloud parameters was used as a starting point for this research. In the existing study, a set of ice accretions were produced in the NASA Glenn IRT for a matrix of varying spraybar pressures. This created a sensitivity of ice accretion geometry to LWC and MVD variations. Ice tracings from the NASA study were selected and used as templates for the simulated ice accretions of the current research. The simulated ice accretions were constructed with stereolithography and mounted on an 18-inch chord NACA 0012 airfoil model. Aerodynamic wind tunnel testing was conducted in the Illinois wind tunnel to produce a sensitivity of aerodynamic performance to ice accretion geometry. All of the wind tunnel testing was conducted at a Reynolds number of 1.8 x 10^6, which corresponded to a Mach number of 0.18. These data were then correlated to the existing NASA study to obtain a sensitivity of aerodynamic performance to icing cloud parameter variations, specifically changes in LWC and MVD. To extend this research to a "real world" perspective, the sensitivity was modified to include the effects of icing cloud parameter changes on aircraft performance. Lastly, the accuracy of LWC and MVD required to simulate ice accretions capable of discerning measurable and significant changes in airfoil and aircraft performance were determined.

This study attempted to answer the question "How good is good enough?" in regard to icing cloud simulation in icing wind tunnels. The major conclusions of this research are presented as follows. Variations in LWC and MVD had an obvious effect on the geometry of a simulated ice accretion, which in turn affected the aerodynamic performance of the airfoil containing the ice accretion. Over the range of ice accretions tested, the maximum lift coefficient deceased by 50% to 80% from the clean configuration. Additionally, the minimum drag coefficients of the simulated ice accretions were 400% to 2000% above the value for the clean model, and the maximum lift to drag ratio of the airfoil was reduced by 88% to 98%. The variation in LWC and MVD required for a measurable effect on airfoil performance was shown to be small. For example, a variation in LWC of 0.006 g/m^3, or a variation in MVD of 0.3 µm was required to produce an ice accretion that resulted in measurable aerodynamic effects outside of the aerodynamic uncertainty involved in the aerodynamic wind tunnel testing. The variation in LWC and MVD corresponding to a change in C_{lmax} of 0.03 was shown to be ΔLWC = 0.11 g/m^3 and ΔMVD = 4.6 µm. For a change in C_{dmin} of 0.0058 the variation in LWC and MVD were found to be 0.06 g/m^3 and 3.1 µm, respectively. These changes in C_{lmax} and C_{dmin} were based on the simulation accuracy between 2-D and 3-D simulated ice accretions. A very important comment about these results is that they are very dependent on the baseline ice accretion and care should be taken in using them outside this study.

This sensitivity was extended to consider the sensitivity of aircraft performance to icing cloud parameter variations. A simple aircraft model was developed using analytical methods as a first step in the process to relate icing cloud parameter changes to their corresponding changes in aircraft performance. The objective of this sensitivity was to find the ΔLWC and ΔMVD required to produce an ice accretion that would have a significant effect on the stall speed of an aircraft. Significant changes in stall speed were defined to be $\Delta V_{stall} = \pm 0.5$ or ± 3 knots based on the certification standards for transport category airplanes. For $\Delta V_{stall} = \pm 0.5$ knots, the required accuracy in ΔLWC was 0.025 g/m^3, and in ΔMVD was 1.1 µm. For $\Delta V_{stall} = \pm 3$ knots, the required accuracy in

ΔLWC was 0.12 g/m^3, and in ΔMVD was 5.5 μm. As before, it is important to note that these data only show sensitivity around the baseline condition, which was IRT run 49 for this study.

Several recommendations were formed based on lessons learned during the course of this research. First, future research should attempt to better decouple the effects of LWC and MVD. Also, smaller ice accretions should be considered because the sizes of the ice accretions studied in this research were large, and the results of this research might be unique to large ice accretions. A better aircraft model should be developed for a more accurate sensitivity of aircraft performance to icing cloud parameter variations. Additionally, it would be helpful to have a direct one-to-one comparison of flight test data and 2-D wind tunnel data to aid in model development. Finally, a detailed aircraft drag model should be developed so that more aircraft performance parameters can be explored.

Acknowledgments

The authors at the University of Illinois were supported, in part, under NASA Grant NCC 3-852 with Gene Addy as technical monitor. The authors wish to thank Sam Lee and Tom Ratvasky of the NASA Glenn Research Center for their help with the aircraft performance sensitivity.

References

[1]NTSB – Aviation Accident Database, available at http://www.ntsb.gov/ntsb/query.asp (last visited November 30, 2006).

[2]Miller, D., Potapczuk, M., and Langhals, T., "Preliminary Investigation of Ice Shape Sensitivity to Parameter Variations," AIAA-2005-0073, 43rd AIAA Aerospace Sciences Meeting and Exhibit, Reno, NV, January 10-13, 2005.

[3]Miller, D., Potapczuk, M., and Langhals, T., "Additional Investigations of Ice Shape Sensitivity to Parameter Variations," AIAA-2006-0469, 44th AIAA Aerospace Sciences Meeting and Exhibit, Reno, NV, January 9-12, 2006.

[4]Bragg, M. B., Broeren, A. P., and Blumenthal, L. A., "Iced-Airfoil Aerodynamics," *Progress in Aerospace Sciences*, Vol. 41, No.5, pp. 323-418, July 2005.

[5]Papadakis, M., Alansatan, S., and Seltmann, M., "Experimental Study of Simulated Ice Shapes On a NACA 0011 Airfoil," AIAA-99-0096, 37th AIAA Aerospace Sciences Meeting and Exhibit, Reno, NV, January 11-14, 1999.

[6]Papadakis, M., Alansatan, S., and Wong, S., "Aerodynamic Characteristics of a Symmetric NACA Section with Simulated Ice Shapes," AIAA-2000-0098, 38th AIAA Aerospace Sciences Meeting and Exhibit, Reno, NV, January 10-13, 2000.

[7]Kim, H. S. and Bragg, M. B., "Effects of Leading-Edge Ice Accretion Geometry on Airfoil Performance," AIAA-99-3150, 17th AIAA Applied Aerodynamics Conference, Norfolk, VA, June 28-July 1, 1999.

[8]Broeren, A. P., Lee, S., LaMarre, C. M., and Bragg, M. B., "Effect of Airfoil Geometry on Performance with Simulated Ice Accretions Volume 1: Experimental Investigation," DOT/FAA/AR-03/64, 2003.

[9]Roskam, J., and Lan, C. T., *Airplane Aerodynamics and Performance*, DARcorporation, Lawrence, KS, 1997.

[10]Bragg, M.B., and Heinrich, D. C., "Effect of Underwing Frost on a Transport Aircarft Airfoil at Flight Reynolds Number," *Journal of Aircraft*, Vol. 31, No. 6, 1994, pp. 1372-1379.

[11]Raymer, D. P., *Aircraft Design: A Conceptual Approach*, AIAA, Washington, DC, 2nd ed., 1992.

[12]Broeren, A.P., "An Experimental Study of Unsteady Flow over Airfoils near Stall," Ph.D. Dissertation, Department of Mechanical Engineering, University of Illinois, Urbana, IL, 2000.

[13]Gurbacki, H. M., "Ice-Induced Unsteady Flowfield Effects on Airfoil Performance," Ph.D. Dissertation, University of Illinois, Urbana, IL, 2003.

[14]Vickerman, M. B., Choo, Y. K., Schilling, H. W., Baez, M., Braun, D. C., and Cotton, B. J., "Toward an Efficient Icing CFD Process Using an interactive Software Toolkit – SmaggIce 2D," AIAA-2002-0380, 40th AIAA Aerospace Sciences Meeting and Exhibit, Reno, NV, January 14-17, 2002.

[15]Kim, H., "Effects of Leading-Edge Ice Accretion Geometry on Airfoil Performance," M.S. Thesis, University of Illinois, Urbana, IL, 2004.

[16]Olsen, W., Shaw, R., and Newton, J., "Ice Shapes and the Resulting Drag Increase for a NACA 0012 Airfoil," NASA TM-83556, 1984.

[17]Campbell, S. E., "Aerodynamic Performance Sensitivity to Icing Cloud Parameters," M.S. Thesis, University of Illinois, Urbana, IL, 2006.

[18]Ratvasky, T. P., Blankenship, K., Reike, W., and Brinker, D. J., "Iced Aircraft Flight Data for Simulator Validation," NASA TM-2003-212114, 2003.

[19]"Flight Test Guide for Certification of Transport Category Airplanes," FAA Advisory Circular AC-25-7A, 1998.